sustainability

MDPI

Article

Nature-Based Solutions for Cooling in High-Density Neighbourhoods in Shenzhen: A Case Study of Baishizhou

Ying Zheng *, Greg Keeffe and Jasna Mariotti

School of Natural and Built Environment, Queen's University Belfast, Belfast BT7 1NN, UK
* Correspondence: yzheng19@qub.ac.uk

Abstract: These days, high-density cities are facing growing challenges related to the urban heat island (UHI) effect. Greening can be a nature-based solution for UHI effect mitigation. This study aims to evaluate the potential of nature-based solutions to improve the urban living environments in Baishizhou, a high-density neighbourhood in Shenzhen. An integrated 3D visualisation research method was proposed in this study. Rhino 7, Grasshopper, and ENVI-met software were combined to evaluate environment characteristics before and after design, as well as compare differences in the outdoor thermal comfort index and the building surface temperature. The greening design scenarios include adding trees, green roofs, and green facades. The simulations ran for 24 h during the test period from 01:00 to 24:00 on 9 August 2019, which was the hottest day in Shenzhen. Baishizhou was selected as the test area for this study and environmental simulation. Results indicated that (1) vegetation has a positive cooling effect, providing outdoor thermal comfort, while shade "trees" provide significant cooling effects on hot days in tropical and subtropical climates; (2) adding green roofs and green facades to a building can significantly affect the cooling effect.

Keywords: urban heat island effect; nature-based solutions; Shenzhen; greening

Citation: Zheng, Y.; Keeffe, G.; Mariotti, J. Nature-Based Solutions for Cooling in High-Density Neighbourhoods in Shenzhen: A Case Study of Baishizhou. *Sustainability* **2023**, *15*, 5509. https://doi.org/10.3390/su15065509

Academic Editor: Pablo Peri

Received: 16 February 2023
Revised: 17 March 2023
Accepted: 19 March 2023
Published: 21 March 2023

1. Introduction

Accelerated urbanisation has resulted in a variety of issues such as high-rising buildings and aggravated urban heat islands (UHI), which directly threaten the deterioration of the environment for urban residents, becoming increasingly detrimental to the physical and psychological health of urban residents [1–3]. Therefore, it is imperative to develop effective strategies to address these issues.

The concept of nature-based solutions (NBS) are solutions that are inspired by or supported by nature [4–6]. NBS refers to natural "green" solutions that can be used to address social, economic, and environmental sustainability issues simultaneously, and thus to improve cities' resilience to climate change and increase the quality of the living environment of the residents [7–11]. On this basis, NBS has evolved into a concept for integrating a variety of ecosystem-based approaches for addressing a series of problems [12]. For instance, they are being adopted into urban development to mitigate the UHI effect and create healthier neighbourhoods [12]. Moreover, United Nations released a strengthened climate plan in 2020 that emphasises the use of NBS as a means to combat the UHI effect [8]. Many previous studies have found that NBSs, such as trees, vegetation, green infrastructure, green roofs, and green walls can mitigate UHI, improve thermal comfort in and around buildings, and reduce the need for mechanical cooling, while providing numerous quality-of-life and health benefits to urban environments [13–20]. For example, Sung concluded that native tree preservation is effective in reducing the urban heat island effect in Texas, USA. [14]. Wang and Akbari confirmed that the urban vegetation system is crucial for the mitigation and adaptation of the UHI effect through ENVI-met modelling [15]. A Canadian study conducted by Hayes examined the advantages and disadvantages of implementing NBSs in cities and examined the UHI's potential effectiveness in changing climates [16].

A measurement method developed by Amani-Beni showed that large urban parks are able to cool their surroundings in the summer [17]. In densely built-up areas, Kim found that enhancing urban micro-scale thermal conditions could be accomplished with small-scale green infrastructure [18]. Andric et al. took Qatar as a case study to investigate green roofs and walls as a mitigation strategy for reducing extreme heat island effects in buildings on extremely hot days [19]. These studies, developing through research and applications, provide a potential for mainstream nature-based solutions to urban planning [20]. While the topic of urban thermal comfort has garnered increasing attention, the nature-based solutions for addressing this issue in high-density Chinese neighbourhoods has received relatively little discussion.

In China, rapid urbanisation has resulted in the loss of valuable agricultural land, leading to the engulfment of many villages located on the outskirts of cities by urban development. These urban villages (Chengzhongcun in Chinese), known as villages in the city have grown phenomenally during the past four decades [21]. For instance, Shenzhen has 320 urban villages within its administrative area [22]. There were approximately 350,000 houses in these villages, giving rise to 106 million m^2 of floor area. According to Shenzhen Public Security Bureau statistics, there were 4.69 million floating residents in urban villages in 2005, which is 14 times more than the 0.33 million indigenous residents [23]. In these villages, buildings are called "handshake buildings" (Woshoulou in Chinese) due to their close proximity to each other, which has led to overcrowding, poor sanitation, and environmental pollution [24–27]. These environmental issues have also contributed to the UHI effect in these villages. Thus, it is vital to alleviate the heat island effect and improve the living environment in high-density urban areas to address the environmental and health challenges faced by local residents.

In this context, green spaces can play a crucial role in mitigating the urban heat island effect. However, as previously mentioned, finding free spaces within the built environment to be re-purposed for green space is challenging in high-density urban areas such as the urban villages of Shenzhen [28]. To overcome this challenge, nature-based strategies such as green facades and green roofs have emerged as viable alternatives to traditional green spaces with tree planting [29]. Green facades can be covered directly or indirectly with herbaceous or creeping plants grown in planter boxes or on the ground, but sometimes support systems are required, which are called green vertical systems or facade greening systems [30,31]. A green roof is a roof covered with green vegetation and growing medium, also known as an eco-roof, roof garden, or living roof [32]. These strategies not only provide significant cooling effects but also contribute to urban greenery, which is crucial for improving environmental quality and enhancing the well-being of urban residents. By adopting such innovative strategies, it is possible to establish more sustainable and liveable high-density urban areas in China.

However, despite the potential benefits of NBS in high-density urban areas, policymakers commonly reject the value of informal settlements, such as Chinese urban villages, and instead focus on aggressive demolition and redevelopment programs aimed at replacing these areas with formal urban neighbourhoods [22]. This lack of exploration of NBS strategies in Chinese urban villages is particularly concerning. Therefore, there is a critical need to explore and promote the use of NBS in Chinese urban villages before they are lost to urbanisation. More case studies are needed to showcase the potential benefits of NBS in high-density urban areas and overcome barriers to implementation, such as limited availability of space for green infrastructure.

This paper proposes the implementation of NBS planning to mitigate the UHI effect and cool high-density urban areas, with a focus on improving outdoor thermal comfort and reducing building surface temperature in Chinese neighbourhoods. The core research question is how to design a high-density neighbourhood that can effectively address the thermal environment. To address this issue, a programmatic design outline is proposed, which identifies key strategies for mitigating the thermal environment through building and street greening. To assess the effectiveness of these strategies, simulation methods are utilised to compare the original model with the proposed design model. The implementation of NBS planning can help address the research gap in exploring nature-based strategies in Chinese high-density neighbourhoods, ultimately contributing to the creation of a more sustainable and comfortable urban environment.

2. Materials and Methods

2.1. Case Study

This study takes place in Shenzhen (113°510 E–114°210 E, 22°270 N–22°390 N), China's first special economic zone (SEZ). Shenzhen is a continually growing megacity with a population of 17.56 million in 2020 [33]. Shenzhen has a subtropical climate, with mild winters and hot and humid summers [34]. According to the Shenzhen Climate Bulletin, the highest temperature was 36.1 °C on 9 August 2019, which was the second highest in the last 10 years and the third highest since 1953. The average annual temperature is 24 °C [34]. The case study area is located in the Baishizhou of Shenzhen, China, which has the highest density urban village without plants (Figure 1). Within the case study site, buildings cover a total of 57.41% of the surfaces, with heights ranging from 9 m to 24 m, which is typical of residential areas in urban villages. This area faces a variety of urgent and typical social and environmental issues arising from morphological diversity, building intensification, population structural changes, and media attention. This study focuses on outdoor thermal comfort and exterior building surface temperature. To explore outdoor thermal comfort, the study used test area simulation. Furthermore, exterior building surface temperatures were extracted from different locations within the test area: Building No. 1 and Building No. 2. Building No. 1 within the test area has a height of 17 m and a floor area of 168 m^2. Building No. 2 is located at the entrance of the test area and has a height of 16 m and a floor area of 168 m^2.

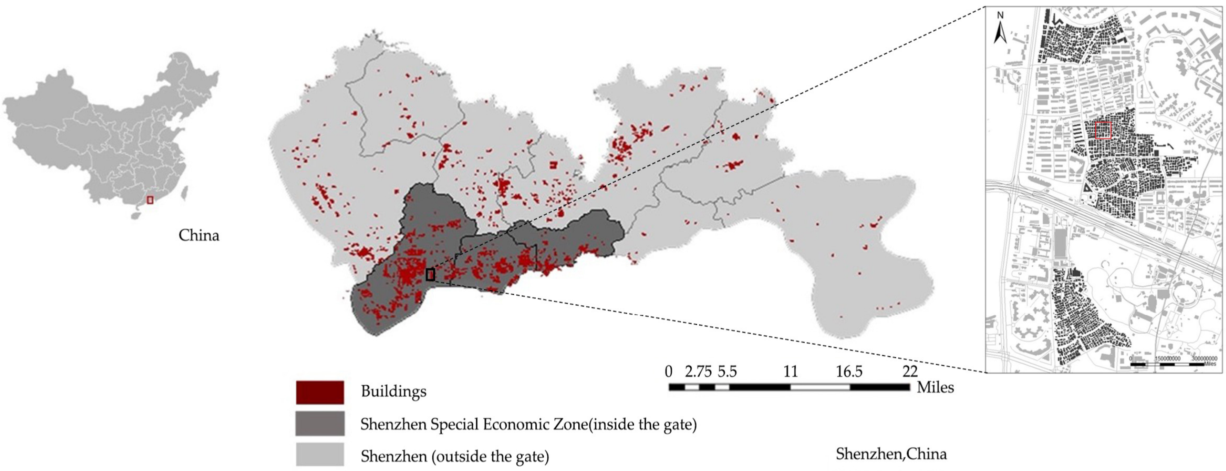

Figure 1. Map of Shenzhen City (**left**) and sample area (**right**) (Source: Baidu Map).

2.2. Method Review

To evaluate the cooling effect of nature-based solutions in urban villages, a three-dimensional modelling simulation approach is necessary due to limitations in measurements. Environmental simulation studies commonly use software such as EnergyPlus, computational fluid dynamics (CFD), ENVI-met, etc. [1]. ENVI-met is a holistic microclimate model developed by Professor Michael Bruse in Germany [35,36]. This microclimate model is designed to calculate the microclimate of an area using CFD packages based on thermodynamics and heat transfer [37]. It allows users to optimise sustainable living conditions in rapidly changing environments. With ENVI-met, multiple elements and climate factors are used to assess the urban environment at a fine scale. It includes simulations of airflow around buildings, air temperature, exchanges of heat and water vapor between the ground and the building surfaces, turbulence, transpiration of vegetation, short-wave radiation, and bioclimatology, etc. [37]. Compared to other software, ENVI-met is regarded as the best fluid mechanics simulation software for outdoor thermal environments [38]. Many researchers have verified that the ENVI-met simulated results are more accurate and closer to actual measurements [39]. Hence, ENVI-met is a useful tool for assessing the impact of nature-based solutions on the environments of urban villages.

2.3. Method Workflow

This study proposes an integrated 3D visualisation research method using the software combination of Rhino 7, Grasshopper, and ENVI-met (Figure 2). Rhino 7 is a powerful 3D modelling software that offers a wide range of tools and features for designers and engineers [40]. Grasshopper is a "graphical algorithm editor" plugin for Rhino 7 [40]. The original 3D model generated the geometry of the buildings with Grasshopper and converted them into ENVI-met buildings using Dragonfly, a plugin of Grasshopper [41,42]. This method was selected because it allows for model variations, enabling changes to the materials or shape of buildings in just a few seconds without having to rebuild the model from scratch [41,42]. Furthermore, this plugin was developed to ensure ENVI-met's functionality while avoiding the limitations of its applicability to microscale simulations and interconnection with an external tool. It utilises the parametric platform of Grasshopper 3D to connect various validated simulation engines, i.e., EnergyPlus, OpenFOAM, Radiance and Daysim, with an easy-to-handle graphical algorithm interface, which allows designers to manipulate design modifications according to the model's environmental performance [42]. This integrated approach helps in the investigation of the outdoor microclimate of the built environment and in the assessment of thermal comfort for a specific period of the year in a relatively small simulation time, which is a substantial factor for urban form finding and optimisation process through different design iterations.

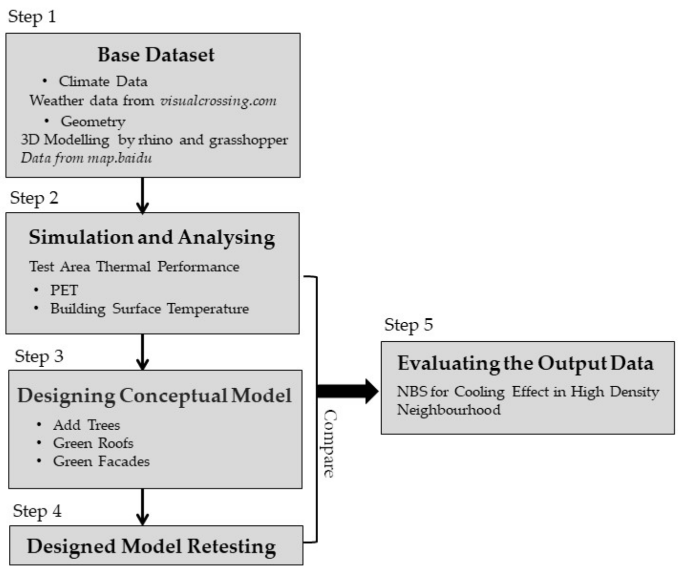

Figure 2. Method Workflow.

Initially, the ENVI-met microclimatic model is configured in Grasshopper using a set of designated modules that automatically translate the input data into Area Input (.INX) and Simulation (.SIM) files. These data include the 3D model of the building, as well as the climatic data for Shenzhen. Building information and climatic data are acquired separately from the Baidu map and Visual Crossing. After collecting the data, the same weather conditions are simulated in the original model. Both simulations are run for 24 h on 9 August 2019, which was the hottest day of the year in Shenzhen. The test period is from 01:00 to 24:00.

This method process combines parametric design and simulation to optimise thermal performance in a high-density neighbourhood (Figure 2). Firstly, this study evaluates the

ENVI-met (version 5.0.3) model in the test area. Secondly, a comparative microclimate analysis in the test area is conducted, which guides climate adaptation. Finally, proposed design ideas are retested. By retesting and refining, a satisfactory solution can be achieved.

2.4. Scenario Design

The study considered two scenarios: the base model and the designed model, both of which were created using Rhino 7 and Grasshopper. The base model included conventional building materials such as concrete roofs, brick walls, and cement concrete pavements commonly found in the case study site. In contrast, the designed model incorporated NBSs such as trees, green roofs, and green facades.

To design the green roofs and facades, an ivy cover was added to the entire building surface of the base model. For streetscape design, bluebell as one of the common arbour species in South China was selected as the three-dimensional trees. The study compared the existing materials with the improved optimal design, as shown below (Table 1).

Table 1. The comparison of existing and improved optimal design of materials.

Classification	Existing Material		Improved Material	
Pavements	Concrete		Stone outdoor paving with grass texture seamless	
Building Roofs	Clay and Brick Tiles		Green Roofs with Ivy	
Building Facades	Ceramic Tiles + Brick Walls		Green Facades	

2.5. Modelling of the Original Area and Designed Area

The SPACES module of ENVI-met 5.0.3 software was used to model the test area of Shenzhen Baishizhou urban village (Figure 3). Model information includes initial environmental parameters (Table 2) and designed parameters (Table 3).

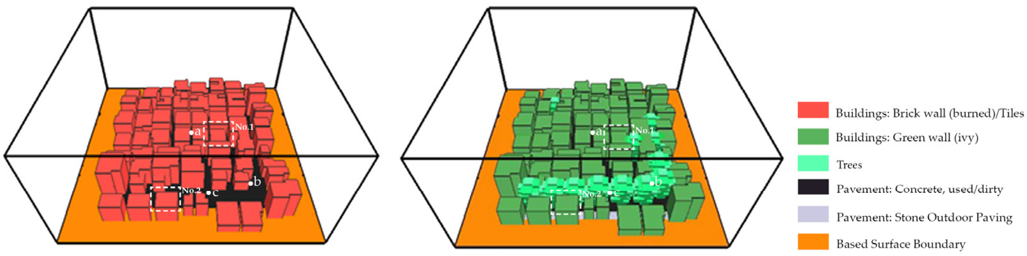

Figure 3. Original model (**left**) and designed model (**right**).

Table 2. Input parameters for ENVI-met modelling.

Simulation Settings
Simulation Input Data Geographic Location (Latitude, Longitude): 22.5, 114.10 Reference time zone: GMT + 8 Simulation Model Size (m): 162 m (L) × 162 m (W) × 88 m (H) Simulation Model Area (Number of Grids) xyz-Grids: 85 × 85 × 44 Size of grid cell (meters) x, y, z: 2 × 2 × 2 Method of vertical grid generation: Equidistant
Main Model Parameters Simulation Model Date: 9 August 19 Start and Duration of Simulation: 01:00, 24 h Initial Wind Speed: 3.3 m/s Wind Direction: 184° Initial Temperature: 28 °C Initial Relative Humidity (%): 77.23%
Model Materials and Properties
Building Materials Original Model: [0100B2] BRICK WALL (Burned): 0.24 m (Substrate Thickness) Designed Model: [0100IV] Ivy (Hedera helix): 0.12 m (Plant Thickness), 0.24 m (Substrate Thickness) Pavements Original Model: [0100ST] Asphalt Rd, [0100PP] Pavement (Concrete), used/dirty Designed Model: [0100KK] Brick Road (Red stones) Albero Designed Model: [020031] Bluebell Tree (middle)

Table 3. Plant species parameter.

3D Plant Species	**Simulation Trees Scenarios**	**Values**
Bluebell (middle)	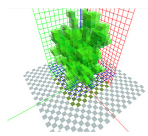	Height (m): 18.42 Width (m): 10.64 × 10.66 LAD (August): 1.00 Number of trees: 12

1. Setting the initial environmental parameters: environmental parameters were obtained from the Visual Crossing website (Figure 4). To address the adverse effects of excessive heat during the summer, particularly in densely populated urban areas, the study day was set to 9 August 2019, the hottest day of the year. To ensure data stability, the simulation period was set from 01:00 a.m. to 24:00 p.m. on the case study day, for a duration of 24 h. Based on the actual site size, the X, Y, and Z axes of the model were set at 85, 85, and 44 grids with a two-meter resolution, respectively. A mesh size of 2 × 2 × 2 was set to provide a sufficient resolution for the analysis within a reasonable timeframe, given the computing resources and the required level of detail [43]. To reduce the influence of boundaries, the Z-axis height within the simulation range was set to be more than twice as high as the top-height building within the simulation range [43]. Consequently, 44 grids were set along the Z-axis. The detailed simulation parameters are shown in Table 2.
2. Setting the designed parameter: designed model comprises 3D trees, facade, and roof greening, with relevant information derived from the planting design completion figure. Plant properties are provided as input parameters, as outlined in Tables 2 and 3.

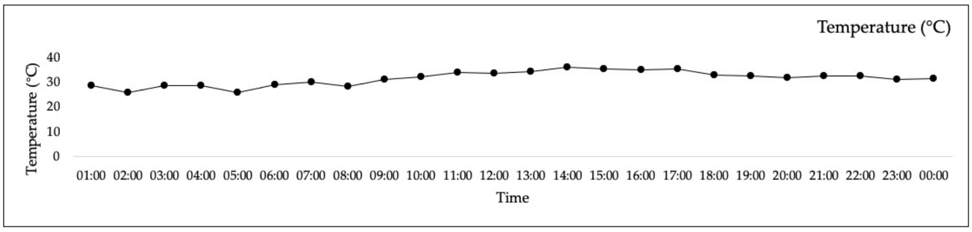

(**a**)

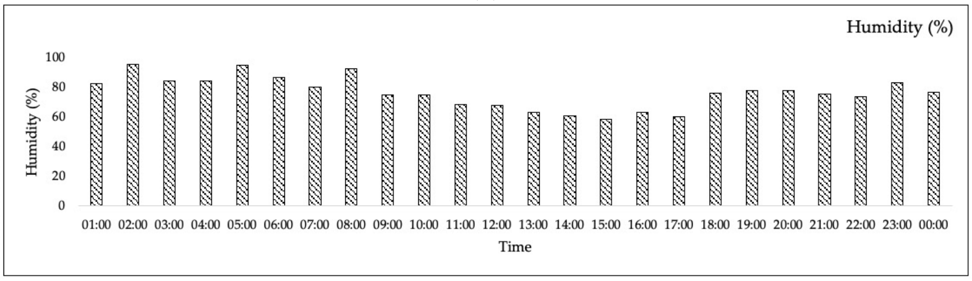

(**b**)

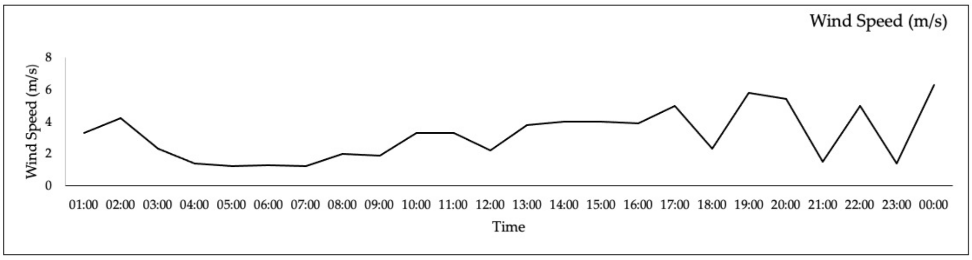

(**c**)

Figure 4. (**a**) Temperature, (**b**) humidity, and (**c**) wind speed on the 9th of August 2019.

2.6. Outdoor Thermal Comfort Indices

"Thermal comfort" reflects a state of mind that expresses satisfaction with a given environment, reflecting both the thermophysiological balance and the body's heat balance [44,45]. Outdoor comfort plays a crucial role in evaluating a city's liveability and promoting people's health [46]. Outdoor human comfort can help urban planners and build designers create more sustainable urban environments, especially in extreme climates [46].

A thermal comfort index is calculated by considering a variety of environmental variables, including air temperature, relative humidity, wind speed, mean radiant temperature, and two personal factors (clothing insulation and metabolic activity level) [47]. Previous studies have developed several different types of thermal comfort indices including predicted mean vote (PMV), physiological equivalent temperature (PET), and universal thermal climate index (UTCI) [48]. PMV is one of the first and most common thermal indices used to assess indoor thermal comfort in buildings with HVAC systems (HVAC stands for heating, ventilation, and air conditioning) [49]. Over the course of this long period of time, however, multiple experimental studies covering several different applications have questioned PMV's accuracy and reliability for all building applications [49]. Comparatively, PET and the UTCI have been found to be more reliable. PET is another rational index, measuring four environmental variables (airflow, air temperature, radiant temperature, and humidity) while keeping clothing and activity rate constant [50]. PET is preferred over index evaluations by the PMV, since it uses a measurement unit (°C), making it convenient for designers and planners to understand without an advanced understanding of meteorology [51]. PET is particularly well-suited for assessing outdoor thermal comfort because it incorporates both short-wave and long-wave radiation fluxes of outdoor spaces [52]. Meanwhile, the UTCI provides one of the most comprehensive heat stress indices for outdoor spaces, as it calculates an equivalent temperature based on a reference environment. The reference environmental temperature that causes strain takes into account dry temperature, relative humidity, solar radiation, and wind speed [53]. Although the UTCI is a useful calculation method for thermal comfort, ENVI-met does not recommend using the UTCI in the regression-based version based on using 2 m (1.6 m) level wind speeds extrapolated to 10 m [54]. Therefore, PET was selected as the thermal comfort index for this case study.

PET calculations are based on simulation data provided by Bio-met, a plugin in ENVI-met. The calculate equation is derived from the energy balance equation between the human body and the environment, known as the Munich Energy-balance Model for Individuals (MEMI) [55]. The PET value represents the air temperature equivalent at which a person (male, 35 years; 1.75 m, 75 kg) would feel the same as under actual circumstances (work activity 80 W, clothing heat resistance Iclo = 0.9, radiant temperature equal to air temperature (Tmrt = T), velocity 0.1 m/s, water vapor pressure 12 hPa) if they were indoors and not active. A PET value is used as an indicator of a person's thermal sensation [56]. Table 4 displays the PET range, which indicates a comfortable range between 18 °C and 23 °C. PET values above or below this range indicate hot or cold discomfort, respectively.

Table 4. Physiologically equivalent temperature (PET) range.

PET(°C)	Thermal Sensation	Physiological Stress Level
<4	very cold	extreme cold stress
4–8	cold	strong cold stress
8–13	cool	moderate cold stress
13–18	slightly cool	slight cold stress
18–23	comfortable	no thermal stress
23–29	slightly warm	slight heat stress
29–35	warm	moderate heat stress
35–41	hot	strong heat stress
>41	very hot	extreme heat stress

2.7. Building Surface Temperature

The thermal conditions of building facades are essential parameters for urban environmental analysis. Local microclimates can have significant effects on the surrounding areas and building facades, affecting the thermal environment, air quality, energy consumption, urban heat islands, and external temperatures [57–59]. In contemporary constructions with good insulation, building facades tend to deteriorate according to the exterior surface microclimate, as external weather conditions change rapidly within short periods of time [59]. Therefore, monitoring surface temperature is a valuable tool for assessing the thermal performance of buildings and implementing them directly or indirectly in virtual simulations [60]. Furthermore, it has significant applications in the field of building physics as a resource for complex analyses of specific thermal phenomena [60].

Building surface temperature can be estimated using ENVI-met. ENVI-met is an advanced model that uses three-layer wall models to provide detailed physics analysis of buildings and more accurate outdoor and indoor simulations [59]. The accuracy of ENVI-met in predicting surface temperatures in urban areas has been validated by some studies.

3. Results

The simulation results are discussed from two perspectives: (1) thermal comfort analysis based on the PET model prediction and (2) analysis of exterior building surface temperature.

3.1. Thermal Comfort Results

The PET index indicates that the thermal perception is in a state of heat stress most of the time. The comfort zone, defined as a temperature range between 18 °C and 23 °C based on physiological equivalent temperature (PET). Extreme heat stress is above 41 °C.

Outdoor thermal comfort was evaluated at three pedestrian level (1.4 m) locations ("a", "b", "c"), as shown in Figure 5. Point "a" is situated in the centre of the test area. Point "b" is located east of the test area next to the building. Point "c" is in front of the entrance to the south of the test area. Simulation results using the base model showed in Figure 6 that PET values at point "a" exceeded 41 °C (extreme heat stress) between 12:00 p.m. and 15:00 p.m. At point "b", PET values were above 41 °C between 9:00 a.m. to 16:00 p.m. At point "c", PET values exceeded this threshold between 9:00 a.m. to 15:00 p.m. However, the cooling effect of NBSs can improve outdoor thermal comfort in a variety of locations. For example, the presence of green facades with ivy reduced PET values by 11.6 °C to 13.5 °C in the morning (around 9:00–11:00) at point "b". Additionally, shade from trees reduced the largest PET value at 9:00 at point "c" by 16.2 °C. However, the PET results indicated that the cooling effect at point "a" was limited because this location was situated on a narrow passage between buildings in the centre of the test area, which caused problems with smooth airflow. Furthermore, it can be note that the cooling effect on the thermal comfort by green roofs and green facades was not significant.

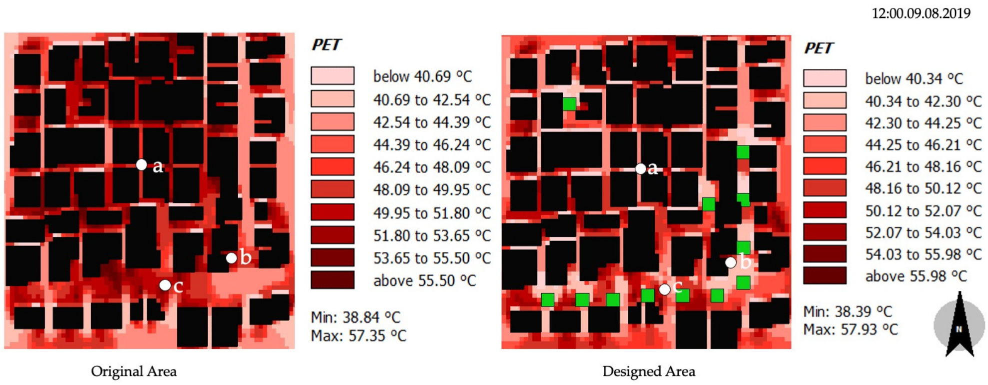

Figure 5. Original area model (**left**) and designed area model (**right**).

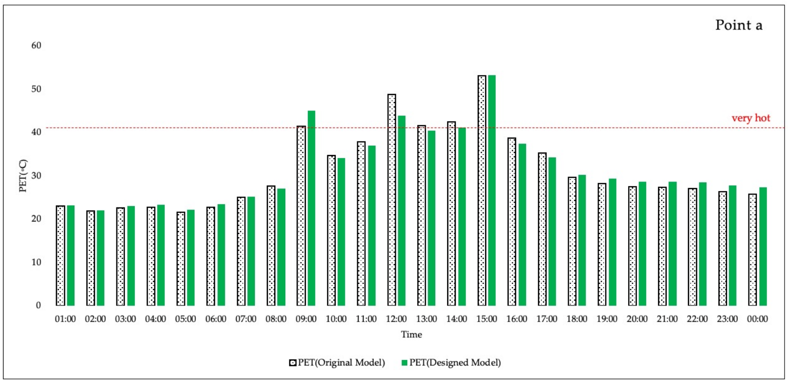

(**a**)

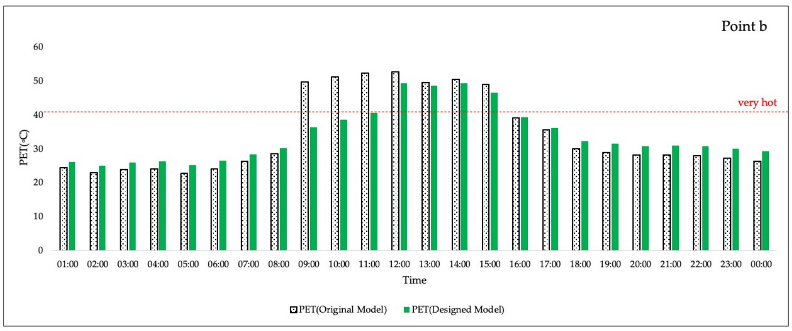

(**b**)

Figure 6. *Cont.*

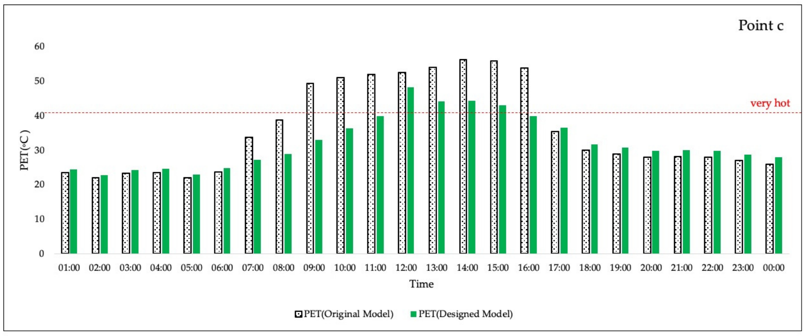

(**c**)

Figure 6. PET values at different points. (**a**) PET value at point "a"; (**b**) PET value at point "b"; (**c**) PET value at point "c".

3.2. Exterior Building Surface Temperature

This section presents the results of ENVI-met simulations, which demonstrate the cooling effect of greening building facades and roofs on surface temperatures across various orientations. Data from the simulation output for the entire case study day was extracted, and the maximum facade cooling effect during the peak solar hour is shown in Figure 7. Figure 7 also displays the distribution of facade surface temperature reduction at 12:00 p.m. resulting from facade and roof greening. For discussion purposes, the two buildings at different locations were extracted and shown (Figures 8–11). Figures 8 and 10 provide 3D visualisations of the building models (bare building model and designed building model).

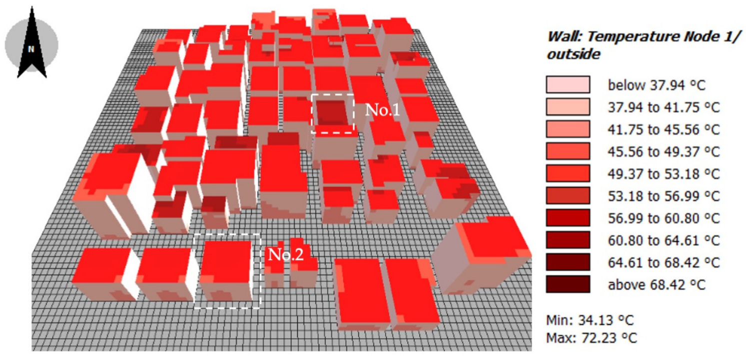

(**a**)

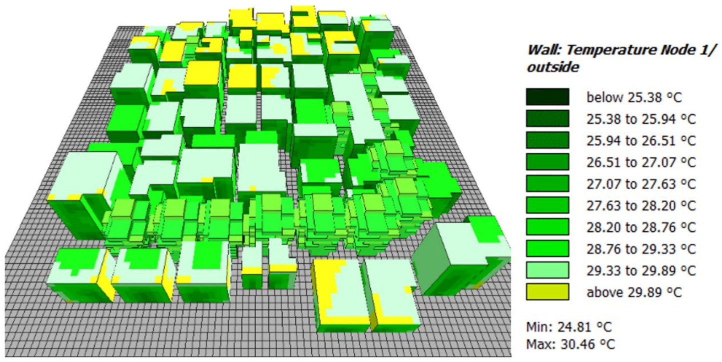

(**b**)

Figure 7. *Cont.*

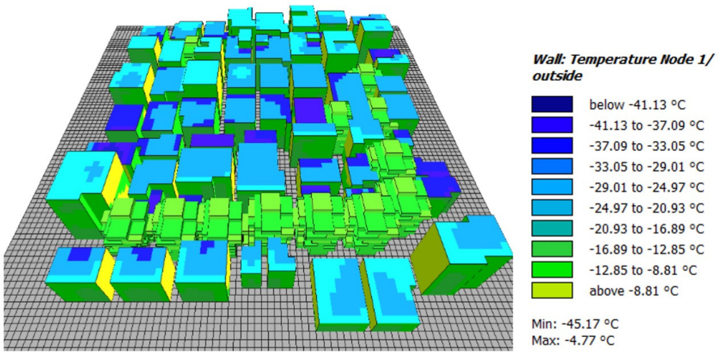

(**c**)

Figure 7. (**a**) Exterior building surface temperatures of the original model; (**b**) exterior building surface temperatures of the designed model; and (**c**) exterior building surface temperatures difference between the original and designed model.

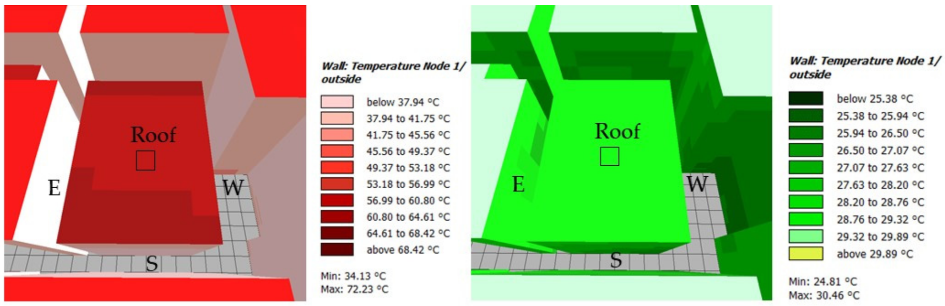

Figure 8. The difference between exterior building surface temperatures of the original model (**left**) and the designed model (**right**) at 12:00 p.m. (building No. 1).

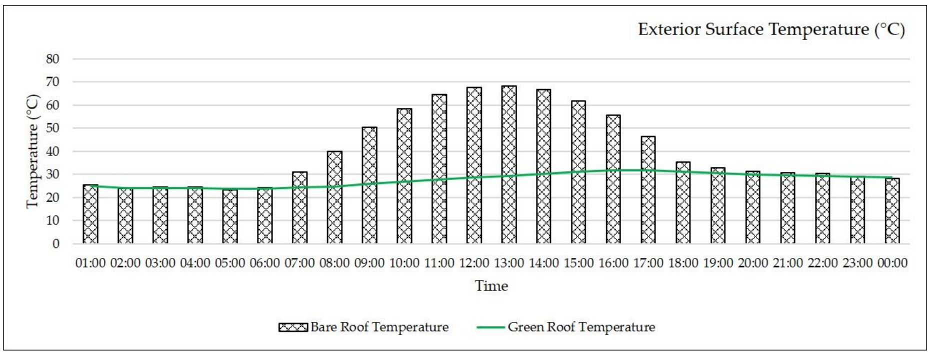

(**a**)

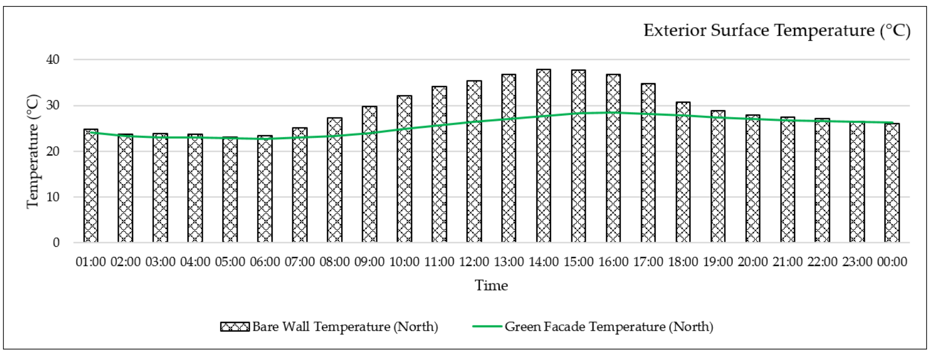

(**b**)

Figure 9. *Cont.*

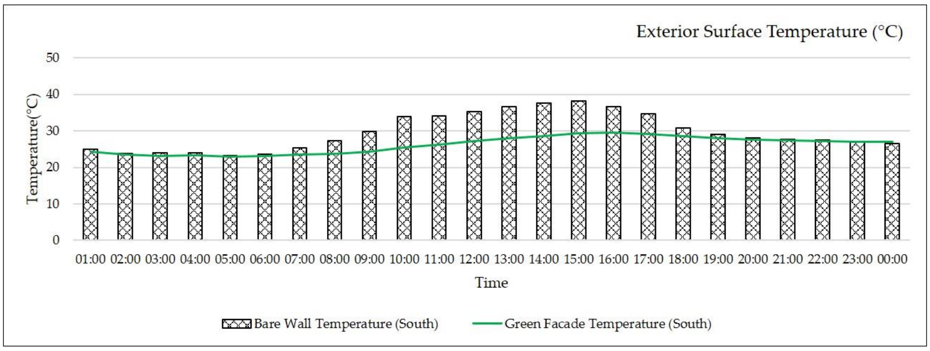

(**c**)

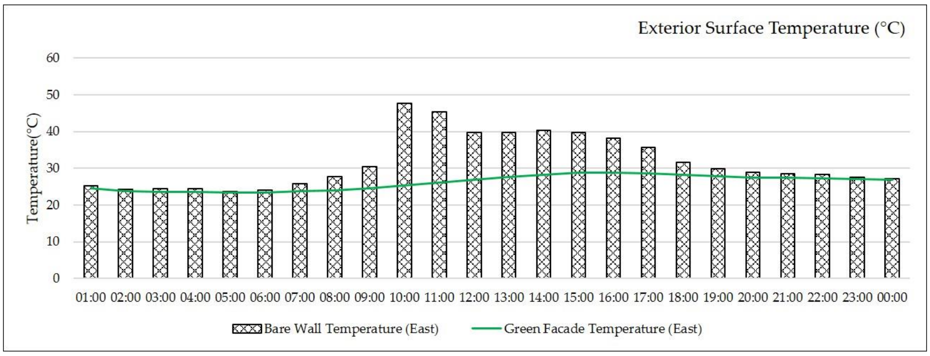

(**d**)

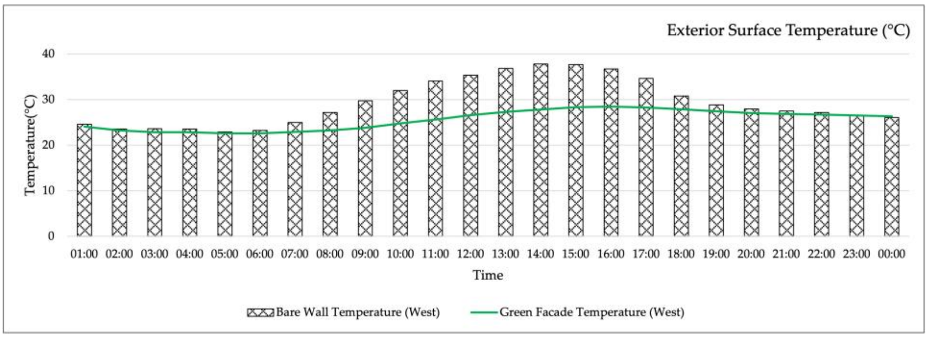

(**e**)

Figure 9. The difference between original Building No. 1 and green Building No. 1. (**a**) Bare roof temperature vs. green roof temperature; (**b**) bare wall temperature vs. green facade temperature (north); (**c**) bare wall temperature vs. green facade temperature (south); (**d**) bare wall temperature vs. green facade temperature (east); (**e**) bare wall temperature vs. green facade temperature (west).

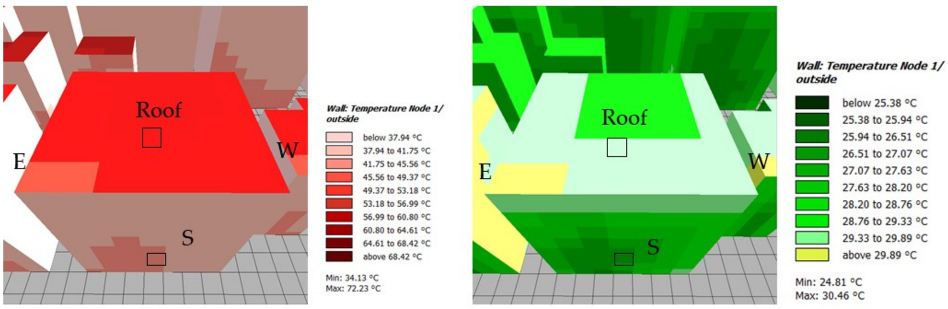

Figure 10. The difference between exterior building surface temperatures of the original model (**left**) and the designed model (**right**) at 12:00 p.m. (building No. 2).

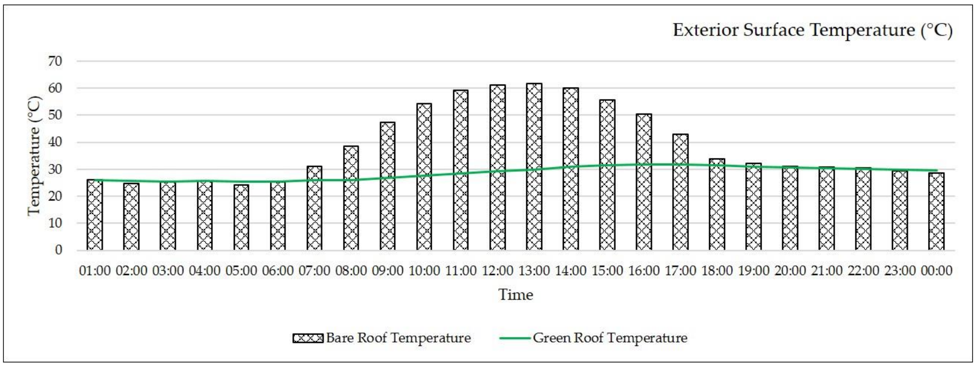

(**a**)

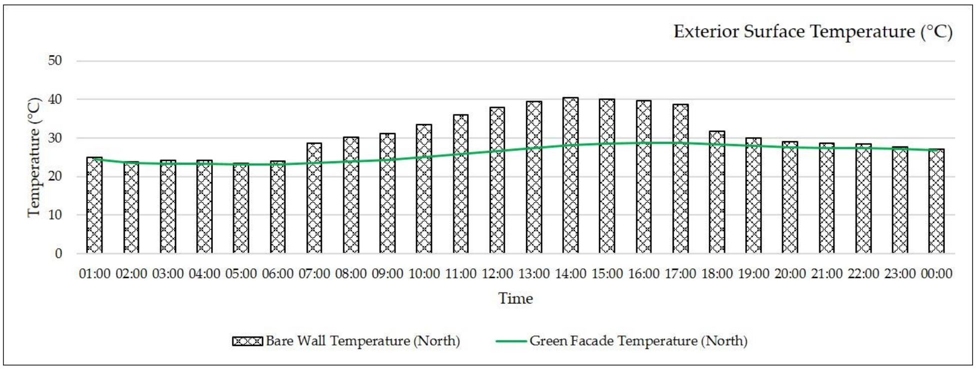

(**b**)

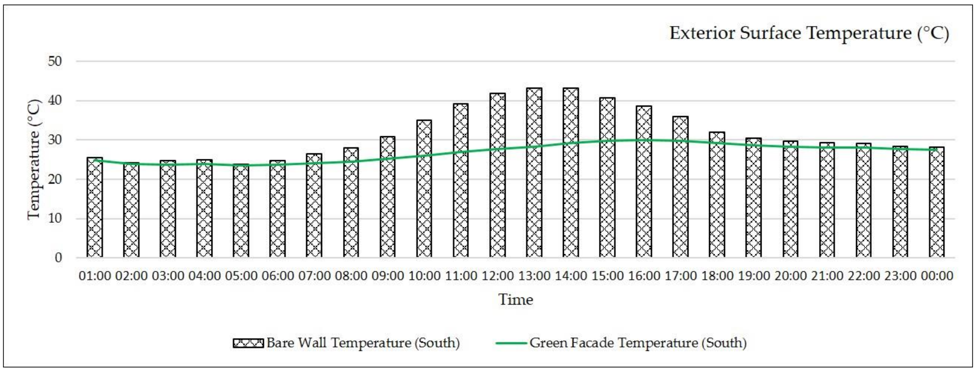

(**c**)

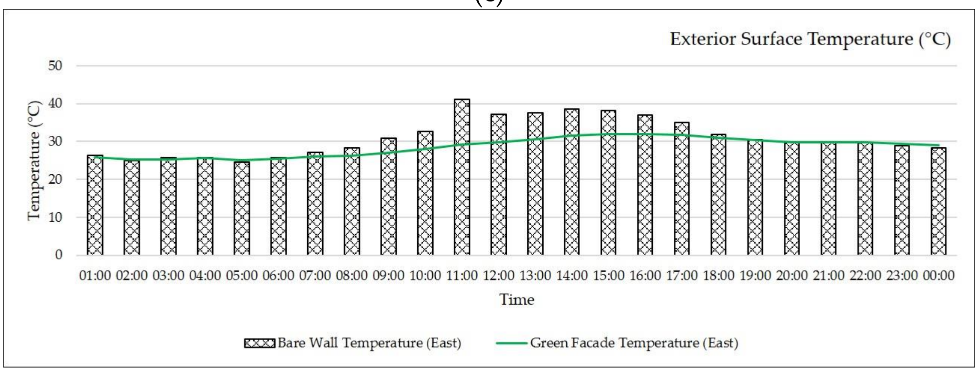

(**d**)

Figure 11. *Cont*.

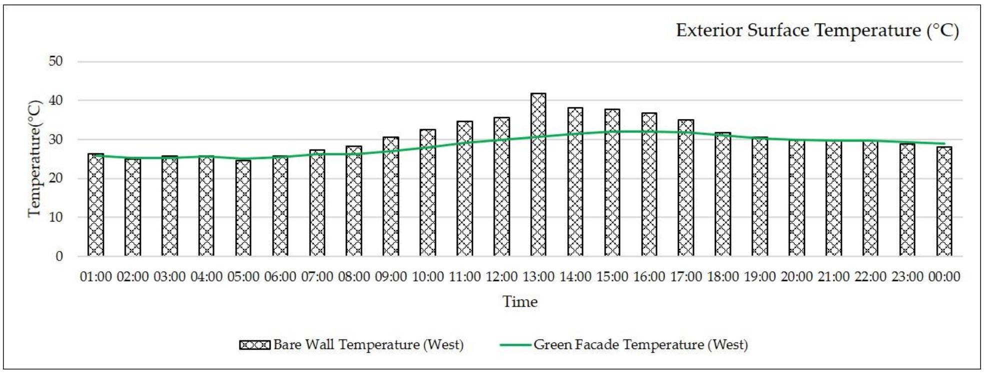

(**e**)

Figure 11. The difference between original Building No. 2 and green Building No. 2. (**a**) Bare roof temperature vs. green roof temperature; (**b**) bare wall temperature vs. green facade temperature (north); (**c**) bare wall temperature vs. green facade temperature (south); (**d**) bare wall temperature vs. green facade temperature (east); (**e**) bare wall temperature vs. green facade temperature (west).

Building No. 1 reached its peak temperature of 68.3 °C at 13:00 p.m. in the test area. The application of a green roof led to a maximum reduction of up to 37 °C in the period (Figure 9). The east-facing facade demonstrated a greater cooling effect than the west-facing facades, owing to their increased exposure to solar radiation before noon (Figures 8 and 9). Notably, the maximum reduction of 22 °C was achieved on the east-facing facade at 10:00 a.m. (Figure 9).

Surface temperature trends in Building No. 2 are similar to those in Building No. 1. Building No. 2 reached its highest temperature of 61.6 °C at 13:00 p.m. in the test area (Figure 11). When the roof was greened, it gives the maximum reduction of 31.6 °C (Figure 11). There is a significant difference in the cooling effect contrast between the facades of the two buildings during the daytime, which is related to solar radiation. Building No. 2 has a greater cooling effect than Building No. 1, which can be attributed to its higher solar exposure. On the contrary, Buildings No. 1 is in shadow due to its narrow distance between adjacent buildings. These findings are illustrated in Figures 10 and 11.

In summary, the installation of green roofs and walls on the exterior of buildings can significantly enhance cooling performance, as shown by the results. The findings demonstrate that (1) exterior building surface temperatures can be reduced by as much as 37 °C; (2) green roofs have a maximum cooling effect of up to 37 °C on test buildings; (3) the cooling effect varies based on the orientation of the greened facade, with Building No. 2 exhibiting more significant cooling effects than Building No. 1; and (4) detecting cooling effects at night is challenging.

4. Discussion

These findings emphasise the importance of combining tree planting and building greening in urban design to optimise thermal comfort in high-density neighbourhoods. It is worth noting that there are four different aspects of the results that are discussed below, providing further insight into the effectiveness of NBS in improving thermal comfort in urban areas.

4.1. NBS for the High-Density Neighbouthood

The study was conducted in a high-density urban village with a complex environment to investigate the potential of NBS planning to improve the thermal environment. This study highlights the influence of outdoor thermal comfort and building surface temperature on the UHI effect and suggests that NBS strategies are effective in mitigating this effect. The findings indicate that incorporating trees into urban design has the greatest impact on improving outdoor thermal comfort, while green roofs and green facades are more effective in reducing building surface temperatures. NBS strategies of tree planting, green roofs, and facades can reduce the UHI effect and optimise thermal comfort for the test area during one of the hottest days in Shenzhen.

4.2. Scenario Simulation Method for the Case Study

This investigation of outdoor thermal comfort involved three crucial components: modelling, scenario design, and simulation. Rhino 7 and Grasshopper were used for modelling and were linked to ENVI-met, which was employed to simulate urban environments and evaluate thermal comfort. The study used the ENVI-met education version 5.0.3 to simplify multiple simulations by using various 3D modelling scenarios in an integrated 3D visualisation research method.

4.3. Adding Trees Have the Greatest Positive Impacts on Outdoor Thermal Comfort

Adding trees to streets can improve outdoor thermal comfort. Trees reduce the amount of short- and long-wave radiation fluxes that impact pedestrians and can significantly lower outdoor temperatures, depending on the type and location of the plant [42]. In this case study, 12 bluebell trees were added to the ground level due to limited land availability. The simulations showed that trees have a limited and localised benefit around the areas covered by their foliage. There is a strong correlation between this benefit and the area shaded by trees. The maximum reduction in the PET index in this study was 16.2 °C at point "c", the entrance of the test area.

4.4. Introduced Facade and Roof Greening into the High-Density Area to Alleviate the Building Surface Temperature

Despite the fact that green roofs and green facades can improve outdoor thermal comfort, the effect may not be significant. Nevertheless, the range of influence of green roofs and green facades on pedestrian-level thermal comfort resulting from this case study can be considered low. Green roofs and green facades, however, are beneficial for reducing building surface temperatures, with a maximum reduction of 37 °C. It is also important to note that the cooling effect of building exterior walls varies in intensity and is affected by the orientation of the building.

5. Limitations

There are several limitations to the case study that need to be considered. Firstly, there are certain limitations regarding the thermal behaviour of building materials and vegetation selected, which can significantly impact outdoor thermal comfort and building surface temperature. This is due to the fact that the model assumes a single material, which is not reflective of reality. Moreover, the simulations were conducted based on a typical hottest day in the subtropical time zone of Shenzhen, which may not be representative of other seasons or climate zones in China. Finally, it is worth noting that population density, which can have a substantial impact on thermal conditions, has not been accounted for in the model.

6. Conclusions

This paper highlights the role of NBSs for high-density urban areas through a case study in the urban village of Shenzhen. The present study focussed on a high-density urban village with a complex environment. Using a combination of numerical simulations, the study demonstrates that NBS planning in a test area can improve the thermal environment by exploring the influence of outdoor thermal comfort and building surface temperature on the UHI effect. The method used Rhino 7, Grasshopper, and ENVI-met integrated 3D visualisation software to simplify multiple simulation scenario analyses.

Simulation results for the current scenario and the designed scenario indicate that NBSs could potentially cool the simulated environment during daytime periods. In high-density urban environments, UHIs can pose significant challenges to the thermal comfort of inhabitants. Thus, NBSs have been identified as a promising approach to addressing this issue. By leveraging natural systems and processes, NBSs can help to mitigate the negative effects of UHIs and improve the thermal environment of urban areas. Specifically, this study found that urban design which combines tree planting and building greening design scenarios can maximise thermal comfort in high-density neighbourhoods. Through these measures, the surface temperature of buildings can be lowered and outdoor thermal comfort can be improved. This finding has significant implications for the design of urban environments, particularly in high-density areas where UHIs are a pressing issue. Furthermore, the proposed method contributes to the implementation of greening schemes in urban development and visualises the potential cooling effects of various design scenarios. Therefore, this study is expected to provide a scientific basis and planning inspiration for the regeneration of urban villages in Chinese megacities.

Future studies will continue to conduct further in-depth investigations on NBS design for high-density urban areas, including vegetation performance analysis in NBS scenarios such as leaf index, growth cycle, maintenance cost, etc. Furthermore, future studies will assess the population density, efficiency, and cost-effectiveness of NBSs in complex urban settings, and explore how to incorporate multiple benefits that nature provides in high-density urban areas. This study provided recommendations for future research directions in Chinese urban villages.

Author Contributions: Conceptualisation, Y.Z. and G.K.; methodology, Y.Z.; software, Y.Z.; writing—original draft preparation, Y.Z.; writing—review and editing, G.K. and J.M.; visualisation, Y.Z.; supervision, G.K. and J.M. All authors have read and agreed to the published version of the manuscript.

Funding: This research was funded by Queen's/China Scholarship Council PhD Scholarships, CSCNO.202010080004.

Institutional Review Board Statement: Not applicable.

Informed Consent Statement: Not applicable.

Data Availability Statement: The data presented in this study are openly available online. Please refer to the website for weather data at https://www.visualcrossing.com/weather-data (accessed on 24 December 2022). Please refer to the website for geographic data at https://map.baidu.com/ (accessed on 24 December 2022).

Conflicts of Interest: The authors declare no conflict of interest.

References

1. Lai, Y.; Ning, Q.; Ge, X.; Fan, S. Thermal regulation of coastal urban forest based on Envi-Met Model—A case study in Qinhuangdao, China. *Sustainability* **2022**, *14*, 7337. [CrossRef]
2. Liu, B.; Lian, Z.; Brown, R.D. Effect of landscape microclimates on thermal comfort and physiological wellbeing. *Sustainability* **2019**, *11*, 5387. [CrossRef]
3. Huang, H.; Deng, X.; Yang, H.; Li, S. Spatial evolution of the effects of urban heat island on residents' health. *Teh. Tech. Gaz.* **2020**, *27*, 1427–1435. [CrossRef]
4. European Commission. *Nature-Based Solutions & Re-Naturing Cities*; European Commission: Brussel, Belgium, 2015; p. 74.
5. Sowińska-Świerkosz, B.; García, J. What are nature-based solutions (NBS)? setting core ideas for concept clarification. *Nat.-Based Solut.* **2022**, *2*, 100009. [CrossRef]
6. Zingraff-Hamed, A.; Hüesker, F.; Lupp, G.; Begg, C.; Huang, J.; Oen, A.; Vojinovic, Z.; Kuhlicke, C.; Pauleit, S. Stakeholder mapping to co-create nature-based solutions: Who is on board? *Sustainability* **2020**, *12*, 8625. [CrossRef]
7. Wickenberg, B.; McCormick, K.; Olsson, J.A. Advancing the implementation of nature-based solutions in cities: A review of Frameworks. *Environ. Sci. Policy* **2021**, *125*, 44–53. [CrossRef]
8. Roggema, R.; Tillie, N.; Keeffe, G. Nature-based urbanization: Scan Opportunities, determine directions and create inspiring ecologies. *Land* **2021**, *10*, 651. [CrossRef]
9. Dorst, H.; van der Jagt, A.; Raven, R.; Runhaar, H. Urban greening through nature-based solutions—Key characteristics of an emerging concept. *Sustain. Cities Soc.* **2019**, *49*, 101620. [CrossRef]
10. Kabisch, N.; Korn, H.; Stadler, J.; Bonn, A. Nature-based solutions to climate change adaptation in urban areas—Linkages between science, policy and practice. In *Nature-Based Solutions to Climate Change Adaptation in Urban Areas*; Theory and Practice of Urban Sustainability Transitions Book Series (TPUST); Springer: Cham, Switzerland, 2017; pp. 1–11. [CrossRef]

11. Roggema, R. From nature-based to nature-driven: Landscape first for the design of Moeder Zernike in Groningen. *Sustainability* **2021**, *13*, 2368. [CrossRef]
12. European Commission. Nature-Based Solutions Generate Greener Urban Renewal. Available online: https://ec.europa.eu/research-and-innovation/en/horizon-magazine/nature-based-solutions-generate-greener-urban-renewal (accessed on 27 December 2022).
13. Balany, F.; Ng, A.W.M.; Muttil, N.; Muthukumaran, S.; Wong, M.S. Green Infrastructure as an urban heat island mitigation strategy—A Review. *Water* **2020**, *12*, 3577. [CrossRef]
14. Sung, C.Y. Mitigating surface urban heat island by a tree protection policy: A case study of the woodland, Texas, USA. *Urban For. Urban Green.* **2013**, *12*, 474–480. [CrossRef]
15. Wang, Y.; Akbari, H. The effects of street tree planting on urban heat island mitigation in Montreal. *Sustain. Cities Soc.* **2016**, *27*, 122–128. [CrossRef]
16. Hayes, A.T.; Jandaghian, Z.; Lacasse, M.A.; Gaur, A.; Lu, H.; Laouadi, A.; Ge, H.; Wang, L. Nature-based solutions (nbss) to mitigate urban heat island (UHI) effects in Canadian cities. *Buildings* **2022**, *12*, 925. [CrossRef]
17. Amani-Beni, M.; Zhang, B.; Xie, G.-D.; Odgaard, A.J. Impacts of the microclimate of a large urban park on its surrounding built environment in the Summertime. *Remote Sens.* **2021**, *13*, 4703. [CrossRef]
18. Kim, Y.; An, S.; Eum, J.-H.; Woo, J.-H. Analysis of thermal environment over a small-scale landscape in a densely built-up Asian megacity. *Sustainability* **2016**, *8*, 358. [CrossRef]
19. Andric, I.; Kamal, A.; Al-Ghamdi, S.G. Efficiency of green roofs and green walls as climate change mitigation measures in extremely hot and dry climate: Case study of Qatar. *Energy Rep.* **2020**, *6*, 2476–2489. [CrossRef]
20. Bush, J.; Doyon, A. Building urban resilience with nature-based solutions: How can urban planning contribute? *Cities* **2019**, *95*, 102483. [CrossRef]
21. Wu, Y.; Zhang, Y. Formal and informal planning-dominated Urban Village Development: A Comparative Study of Luojiazhuang and Yangjiapailou in Hangzhou, China. *Land* **2022**, *11*, 546. [CrossRef]
22. Hao, P.; Sliuzas, R.; Geertman, S. The development and redevelopment of urban villages in Shenzhen. *Habitat Int.* **2011**, *35*, 214–224. [CrossRef]
23. Hao, P.; Geertman, S.; Hooimeijer, P.; Sliuzas, R. Spatial evolution of urban villages in Shenzhen. In *Rural Migrants in Urban China*; Routledge: Oxfordshire, UK, 2013; pp. 202–220. [CrossRef]
24. Tan, X.; Altrock, U.; Schoon, S.; Zhao, J. Localized place-making and the knowledge-based regeneration strategies—The case of Xiasha village in Shenzhen. *Habitat Int.* **2019**, *83*, 73–84. [CrossRef]
25. Chan, K.W.; Zhang, L. The hukou system and rural-urban migration in China: Processes and changes. *China Q.* **1999**, *160*, 818–855. [CrossRef]
26. Wang, Y.P.; Wang, Y.; Wu, J. Urbanization and informal development in China: Urban villages in Shenzhen. *Int. J. Urban Reg. Res.* **2009**, *33*, 957–973. [CrossRef]
27. Zheng, Y.; Keeffe, G. Defining ecological niches for green facades: A case study in Shenzhen, China. In *Ecocity World Summit 2021–22: Conference Proceedings*; Ecocity Builders: Oakland, CA, USA, 2022; pp. 133–141.
28. Rodriguez-Valencia, A.; Ortiz-Ramirez, H.A. Understanding green street design: Evidence from three cases in the U.S. *Sustainability* **2021**, *13*, 1916. [CrossRef]
29. Morakinyo, T.E.; Lai, A.; Lau, K.K.-L.; Ng, E. Thermal benefits of vertical greening in a high-density city: Case study of Hong Kong. *Urban For. Urban Green.* **2019**, *37*, 42–55. [CrossRef]
30. Safikhani, T.; Abdullah, A.M.; Ossen, D.R.; Baharvand, M. A review of energy characteristic of vertical greenery systems. *Renew. Sustain. Energy Rev.* **2014**, *40*, 450–462. [CrossRef]
31. Köhler, M. Green facades—A view back and some visions. *Urban Ecosyst.* **2008**, *11*, 423–436. [CrossRef]
32. Besir, A.B.; Cuce, E. Green roofs and facades: A comprehensive review. *Renew. Sustain. Energy Rev.* **2018**, *82*, 915–939. [CrossRef]
33. Shenzhen Bureau of Statistics. *Data of the Seventh National Census of Shenzhen in 2020*; Shenzhen Bureau of Statistics: Shenzhen, China, 2020.
34. Shenzhen Climate Bulletin 2019. Available online: http://weather.sz.gov.cn/attachment/0/951/951411/6851743.pdf (accessed on 21 December 2022).
35. Bruse, M.; Fleer, H. Simulating surface–plant–air interactions inside urban environments with a three dimensional numerical model. *Environ. Model. Softw.* **1998**, *13*, 373–384. [CrossRef]
36. Srivanit, M.; Hokao, K. Evaluating the cooling effects of greening for improving the Outdoor Thermal Environment at an institutional campus in the Summer. *Build. Environ.* **2013**, *66*, 158–172. [CrossRef]
37. ENVI-Met. Available online: https://www.envi-met.com/ (accessed on 21 December 2022).
38. Fang, X.; Shen, L.; Meng, Q. The study on microclimate simulation of Country Park based on Envi-met software—Take the East Gate entrance area of Guangdong Tianlu lake country park for example. In *Proceedings of the 3rd International Conference on Mechatronics, Robotics and Automation*; Advances in Computer Science Research Series; Atlantis Press: Amsterdam, The Netherlands, 2015. [CrossRef]
39. Yang, J.; Hu, X.; Feng, H.; Marvin, S. Verifying an Envi-Met Simulation of the Thermal Environment of Yanzhong Square Park in Shanghai. *Urban For. Urban Green.* **2021**, *66*, 127384. [CrossRef]
40. Rhinoceros. Available online: Rhino3d.com (accessed on 15 March 2023).

41. Grasshopper 3D. Available online: grasshopper3d.com (accessed on 15 March 2023).
42. Ladybug Tools. Available online: https://www.ladybug.tools/dragonfly.html (accessed on 15 February 2023).
43. Teshnehdel, S.; Gatto, E.; Li, D.; Brown, R.D. Improving outdoor thermal comfort in a steppe climate: Effect of water and trees in an urban park. *Land* **2022**, *11*, 431. [CrossRef]
44. ASHRAE. *Thermal Environmental Conditions for Human Occupancy*; ASHRAE: Atlanta, GA, USA, 2010.
45. Höppe, P. Different aspects of assessing indoor and outdoor thermal comfort. *Energy Build.* **2002**, *34*, 661–665. [CrossRef]
46. Coccolo, S.; Pearlmutter, D.; Kaempf, J.; Scartezzini, J.-L. Thermal Comfort Maps to Estimate the Impact of Urban Greening on the Outdoor Human Comfort. *Urban For. Urban Green.* **2018**, *35*, 91–105. [CrossRef]
47. Shooshtarian, S.; Lam, C.K.; Kenawy, I. Outdoor Thermal Comfort Assessment: A Review on Thermal Comfort Research in Australia. *Build. Environ.* **2020**, *177*, 106917. [CrossRef]
48. Lai, D.; Guo, D.; Hou, Y.; Lin, C.; Chen, Q. Studies of Outdoor Thermal Comfort in Northern China. *Build. Environ.* **2014**, *77*, 110–118. [CrossRef]
49. Laouadi, A. A New General Formulation for the PMV Thermal Comfort Index. *Buildings* **2022**, *12*, 1572. [CrossRef]
50. Gatto, E.; Buccolieri, R.; Aarrevaara, E.; Ippolito, F.; Emmanuel, R.; Perronace, L.; Santiago, J.L. Impact of Urban Vegetation on Outdoor Thermal Comfort: Comparison between a Mediterranean City (Lecce, Italy) and a Northern European City (Lahti, Finland). *Forests* **2020**, *11*, 228. [CrossRef]
51. Elnabawi, M.H.; Hamza, N. Behavioural Perspectives of Outdoor Thermal Comfort in Urban Areas: A Critical Review. *Atmosphere* **2019**, *11*, 51. [CrossRef]
52. Taib, N. Assessment of Physiological Equivalent Temperature (PET) in Transitional Spaces of a High-Rise Building. *Asian J. Behav. Stud.* **2018**, *3*, 13–21. [CrossRef]
53. Zare, S.; Hasheminejad, N.; Shirvan, H.E.; Hemmatjo, R.; Sarebanzadeh, K.; Ahmadi, S. Comparing Universal Thermal Climate Index (UTCI) with Selected Thermal Indices/Environmental Parameters during 12 Months of the Year. *Weather. Clim. Extrem.* **2018**, *19*, 49–57. [CrossRef]
54. UTCI. Available online: https://envi-met.info/doku.php?id=apps:biomet_utci (accessed on 4 January 2023).
55. Höppe, P. The physiological equivalent temperature—A universal index for the biometeorological assessment of the thermal environment. *Int. J. Biometeorol.* **1999**, *43*, 71–75. [CrossRef] [PubMed]
56. Matzarakis, A.; Mayer, H. Another Kind of Environmental Stress: Thermal Stress. WHO Colloborating Centre for Air Quality Management and Air Pollution Control. *Newsletters* **1996**, *18*, 7–10.
57. Tsoka, S.; Tsikaloudaki, K.; Theodosiou, T. Urban Space's Morphology and Microclimatic Analysis: A Study for a Typical Urban District in the Mediterranean City of Thessaloniki, Greece. *Energy Build.* **2017**, *156*, 96–108. [CrossRef]
58. Charisi, S.; Thiis, T.K.; Stefansson, P.; Burud, I. Prediction Model of Microclimatic Surface Conditions on Building Façades. *Build. Environ.* **2018**, *128*, 46–54. [CrossRef]
59. Slávik, R.; Čekon, M. Study of Surface Temperature Monitoring in the Field of Buildings. *Procedia Eng.* **2016**, *161*, 1135–1143. [CrossRef]
60. Forouzandeh, A. Prediction of Surface Temperature of Building Surrounding Envelopes Using Holistic Microclimate Envi-Met Model. *Sustain. Cities Soc.* **2021**, *70*, 102878. [CrossRef]